NOVEMBER 1978 LRP 146/78

OBSERVATION OF THE ABSOLUTE PARAMETRIC DECAY INSTABILITY

R.W. Means, M.Q. Tran[+], and V.P. Silin[++]

[+]University of California at Los Angeles
Department of Physics

[++]Lebedev Physical Institute, Moscow

Observation of the Absolute Parametric Decay Instability

R.W. Means, M.Q. Tran[+], and V.P. Silin[++]

Centre de Recherches en Physique des Plasmas
Ecole Polytechnique Fédérale de Lausanne
CH-1007 Lausanne / Switzerland

[+]University of California at Los Angeles
Department of Physics

[++]Lebedev Physical Institute, Moscow

Abstract

In this paper we present the first experimental evidence of the absolute parametric decay instability realized in a plasma near maxima of the pump field theoretically predicted by Silin and Starodub.

The parametric instabilities in inhomogeneous plasmas are of interest to us in connection with the possibilities of different real applications in the field of laser induced pellet fusion. In this paper we present the first experimental evidence of the absolute parametric decay instability realized in a plasma near maxima of the pump field theoretically predicted by Silin and Starodub[1].

The experiments are performed in a large, cylindrical, unmagnetized, d.c. discharge plasma with a 2m diameter and a 3m length. A density gradient along the axis of the machine can be maintained by controlling the ionizing discharge current from separate groups of filaments. The gradient scale length $L = (\frac{1}{n}\frac{dn}{dx})^{-1}$ can be varied from 200 - 1000 cm. The microwaves are introduced into the chamber at one end by a standard horn antenna with a beam half-angle divergence of 12^{o}. The experiments were performed with a microwave frequency $\nu_o = 2.45 \cdot 10^9$ Hz corresponding to a critical density $n_o = 7.58 \cdot 10^{10}$ particles/cm^3. The electron temperature ratio T_e/T_i was approximately 10. In the experiment the angle, θ, between the microwave beam and the plasma gradient is not well defined because of the divergence of the antenna. The earth's magnetic field also skews the density gradient slightly so that the gradient makes an angle of approximately 10^{o} with the axis of the chamber.

When a continuous medium power microwave beam is incident on the plasma, ion wave fluctuations are observed at both the critical layer and the reflection layer. The incident microwave radiation is primarily p-polarized in this experiment. However, because of the beam divergence of

the antenna and the skew of the density gradient mentioned previously, the microwave beam has a component in the s-plane. The linear theory of the propagation of a plane electromagnetic wave into an inhomogeneous plasma predicts the creation of a standing wave reflected from the plasma layer where the density is given by $n = n_o \cos^2 \theta$. Beyond this layer the electromagnetic wave decays exponentially to zero if the wave is s-polarized. If the wave is p-polarized, then the electric field has a further peak at the critical layer where $n = n_o$. This behaviour can be seen experimentally in Figure 1. The amplitude of the p-polarized wave is enhanced in a zone of the plasma where the S-polarized beam shows only decay. The electric field in this case has been measured in the plasma by means of a neon indicator lamp. This is a new method for measuring microwave fields in a plasma. The high frequency electric field causes an increased conductivity in the abnormal glow discharge in the neon lamp. This increased conductivity can be measured by an increase in the bias current of the lamp. The fundamental sensitivity has been measured in a series of papers by Kopeika et al.[2]. The data shown in Figure 1 only roughly approximates the Airy-function pattern given by linear theory. Nevertheless, the data is sufficient to prove that the two planes where turbulence is seen are the reflection layer and the critical layer. Later we shall use Airy function picture only for our rough estimation.

Figure 2 is a plot of typical ion wave fluctuation levels as a function of incident microwave power. The following parameters are typical of the plasma : $\lambda_D = 3.87 \cdot 10^{-3}$ cm, L = 300 cm, $\gamma_s/\omega_s = 0.035$, $\nu_e/\omega_e = 6.5 \cdot 10^{-5}$, $E_o/4\pi n_o T_e = 10^{-5}$ for P_o = 20W. The fluctuations

were measured using a Langmuir probe biased to collect electrons and integrated from 10 Khz to 10 MHz in a thermal element. The ion plasma frequency at the critical layer was 9 MHz.

The oscillations at the reflection layer have several characteristic features which differentiate them from those at the critical layer. The frequency spectrum at the critical layer as shown in Figure 3a, is of the broadband type without any line. At the reflection layer, however, the frequency spectrum shown in Fibure 3b is of the line type with a peak at 1.5 MHz in this example. With a pulsed source we were able to measure the wavelength in the gradient direction. This will be discussed further later. To rule out the possibility that the line spectra were due to oscillations at the electron cyclotron frequency in the earth's magnetic field, a weak magnetic field was induced by an external coil. The observed frequency was found to be independent of the magnetic field.

These spectral features of the low frequency oscillations at the reflection layer and other maxima of the pump field can be understood on the basis of the formula[1]

$$\left(\frac{\omega}{\omega_{p_2}}\right)^2 = \frac{x}{3L} = \frac{1}{3}\left[\sin^2\theta + \left(\frac{c}{\omega_0 L}\right)^{2/3} |\xi_m|\right] \qquad (1)$$

where x is the separation between the critical layer and the reflection layer, where ξ_m is the coordinate of a maximum of the Airy function, Ai($-\xi$), and θ is the angle of incidence of the electromagnetic wave. This formula correctly describes the position of the frequency peak seen in the spectrum of Figure 3b. In this case for x = 20 cm and L = 300 cm, the calculated frequency peak is 1.3 MHz, which is in close agreement with the experimental value. The formula (1) also

the antenna and the skew of the density gradient mentioned previously, the microwave beam has a component in the s-plane. The linear theory of the propagation of a plane electromagnetic wave into an inhomogeneous plasma predicts the creation of a standing wave reflected from the plasma layer where the density is given by $n = n_o \cos^2 \theta$. Beyond this layer the electromagnetic wave decays exponentially to zero if the wave is s-polarized. If the wave is p-polarized, then the electric field has a further peak at the critical layer where $n = n_o$. This behaviour can be seen experimentally in Figure 1. The amplitude of the p-polarized wave is enhanced in a zone of the plasma where the S-polarized beam shows only decay. The electric field in this case has been measured in the plasma by means of a neon indicator lamp. This is a new method for measuring microwave fields in a plasma. The high frequency electric field causes an increased conductivity in the abnormal glow discharge in the neon lamp. This increased conductivity can be measured by an increase in the bias current of the lamp. The fundamental sensitivity has been measured in a series of papers by Kopeika et al.[2]. The data shown in Figure 1 only roughly approximates the Airy-function pattern given by linear theory. Nevertheless, the data is sufficient to prove that the two planes where turbulence is seen are the reflection layer and the critical layer. Later we shall use Airy function picture only for our rough estimation.

Figure 2 is a plot of typical ion wave fluctuation levels as a function of incident microwave power. The following parameters are typical of the plasma : $\lambda_D = 3.87 \cdot 10^{-3}$ cm, L = 300 cm, $\gamma_s/\omega_s = 0.035$, $\nu_e/\omega_e = 6.5 \cdot 10^{-5}$, $E_o/4\pi n_o T_e = 10^{-5}$ for P_o = 20W. The fluctuations

permits us to offer a possible explanation of the qualitative difference between the spectra of Figures 3a and 3b. Instead of angular independence of the mismatch at the critical point, the mismatch of resonance at the reflective point is, as it is evident from (1), a function of angle θ. So the spectrum of Figure 3b may be a recreation of the antenna pattern of the microwave horn.

We have also seen ion wave fluctuations at an earlier peak of E^2 before the reflection layer. The main peak of the spectrum was at 5 MHz, while the fluctuations at the reflection layer had a spectral peak of 3 MHz. The position of the probe was off the axis of the machine. This confirms that the spectrum of the ion waves is a function of both distance and angle.

Another characteristic of the ion fluctuations is their relatively narrow spatial extent. The width Δx is roughly independent of microwave power and is approximately 5cm. On the other hand the theory[1] predicts the width of the space localization of the fluctuations :

$$\Delta x \approx \left(\frac{v_{Te}}{c}\right)^{1/2}\left(\frac{\omega_0}{\nu_{ei}}\right)^{1/4}\left(\frac{\omega_0 L}{c}\right)^{1/6}\frac{c}{\omega_0} \qquad (2)$$

which, for the experimental parameters, gives us approximately 2cm. This is close to the measured value. Also the theory[1] predicts a standing wave picture in x-direction with the wave length a little less than Δx. This very important feature of the ion fluctuations can be inferred from measurements done in a pulsed experiment. The waves seen in the pulsed

experiment (P_o = 900 W, τ = 2μs) at the reflection layer did not propagate in the x direction. Their wavelength was measured to be approximately 1 - 2 cm. Let us note that the theory of the absolute instability distinguishes between the small x projection of $\underline{k}$ ($k_x \sim 1/\Delta x$) and the larger projection of $\underline{k}$ which is perpendicular to the gradient direction and which determines the frequency of ion oscillation. The large mismatch of the resonance near the turning point gives us not only the large enough frequency of fluctuation but also the high threshold

$$\frac{E_o^2}{4\pi n_o k_B T_e} = \frac{8 \gamma_o \gamma_s}{\omega_o \omega_s} \tag{3}$$

This threshold is close to $2 \cdot 10^{-5}$ and thus about one order lower than the measured threshold if we take into account Airy function enhancement of pumping field

$$E_o^2 = E_{VACUUM}^2 \; 3.7 \left(\frac{\omega_o L}{c}\right)^{1/3} \tag{4}$$

The creation of the ion fluctuation is connected with density depression Δn. These data are shown in Figure 4 and are summarized in Table I. In our treatement of these date we believe that the density depression near the turning point is directly attributed to the level of the Langmuir turbulence.

$$\frac{\Delta n}{n} = \frac{E_L^2}{4\pi n_o k_B T_e} \tag{5}$$

This permits us to speak of the direct measurement of the square of the strength of the longitudinal field which is much higher than the strength of the pumping field. The region of the density depression Δn coincides with the region of low frequency turbulence. However, it is not caused by the low frequency turbulence but the high frequency Langmuir oscillations.

The qualitative description of turbulent fluctuations in our plasma is possible on the basis of the weak turbulence theory[3] because the growth rate

$$\gamma = \frac{1}{4}\left[\omega_o \omega_s \frac{E_o^2}{4\pi n_o k_B T_e}\right]^2 \qquad (6)$$

is less than ω_s and larger than γ_s. Thus for the level of Langmuir turbulence we can use the formula[3] :

$$\frac{E_L^2}{4\pi n_o k_B T_e} = \frac{8\gamma^3}{\gamma_s \omega_o \omega_s} = \alpha \left(\frac{E_o^2}{4\pi n_o k_B T_e}\right)^{3/2} \qquad (7)$$

where $\alpha = (1/8)\ (\omega_s/\gamma_s)\ \omega_o/\omega_s \simeq 200$. If we should use equation (4) for E_o^2 we obtain, as is demonstrated in Table I, an experimental value of α only several times larger than predicted. E_o^2 in equation (7) is the average value. Thus we should compare α for the average value of Δn. Within the range of experimental parameters the ratio, γ/ν_{ei}, is less than a small integer. Thus the numbers of spectral satellites

predicted by the weak turbulence theory[3] is also a small integer. This can give another explanation of the several peaks in the spectrum of Figure 3b, since the theory predicts another main satellite in the ion wave spectrum with the frequency of decay equal to twice the frequency of the main peak. The intensity of the first decay product of the Langmuir spectra is given by the weak turbulence theory to be comparable to the intensity of the primary Langmuir wave. This would imply that the amplitude of the second harmonic acoustic wave would also be comparable to the primary acoustic wave. This is seen to be the case in Figure 2b. The higher harmonics could be due to nonlinear mixing of the two ion acoustic waves. Their amplitude is much smaller. On the other hand, near the critical density layer, the small k values of the primary created Langmuir waves permit us to think about the strong turbulence situation with a practically continuous spectrum.

Thus we have demonstrated the experimental realization of the absolute decay ($t \rightarrow 1 + s$) parametric instability and we have obtained qualitative agreement with linear and nonlinear theoretical predictions.

This work was supported by the Swiss National Science Foundation.

Acknowledgements

We acknowledge many helpful discussions with Drs. K. Appert, R. Bingham, F.F. Chen and J. Vaclavik.

References

1 Silin, V.P., Starodub, A.N., Sov. Journal of Plasma Physics (USA), 3, 156 (1977)

Silin, V.P., Journal de Physique, Colloque C6, Suppl. au no. 12, Tome 38, p. C6-153

2 Kopeika, N.S., Galore, B., Stempler, D., and Heimenrath, Y., IEEE Trans. Microwave Theory Tech. MTT-23, 843 (1975), Makover, Y., Manor, O.R., and Kopeika, N.S., IEEE Trans. Microwave Theory Tech. MTT-26, 39 (1978)

3 Bychekov, V.Yu., Silin, V.P., Tikhonchuk, V.T., JETP Lett. (USA), 26, 197 (1977)

Figure Captions

1. The electric field squared as a function of distance in the plasma. The antenna was rotated 90^{o} in order to observe the two polarizations.

2. The ion fluctuation level at the critical layer and the reflection layer as a funciton of incident microwave power.

3. The spectrum of the ion wave fluctuations for an incident power of 60W , a) at the critical layer, b) at the reflection layer.

4. Density profile modification as a function of incident microwave power.

TABLE I

P_o Watts	$\frac{E^2_{VAC}}{4\pi nkT_e}$	$\frac{\Delta n}{n}$	$\langle\frac{\Delta n}{n}\rangle$	$\frac{E_o^2}{4\pi nkT_e} = \frac{E^2_{VAC}}{4\pi nkT_e} 3.7\left(\frac{\omega_o L}{c}\right)^{\frac{1}{3}}$	$\alpha = \frac{\Delta n}{n} \Big/ \left[\frac{E_o^2}{4\pi nkT_e}\right]^{\frac{3}{2}}$	$\langle \alpha \rangle$
50 W	$2.5 \cdot 10^{-5}$	0.012	0.006	$5 \cdot 10^{-4}$	$1.1 \cdot 10^3$	550.
60 W	$3 \cdot 10^{-5}$	0.019	0.009	$6 \cdot 10^{-4}$	$1.3 \cdot 10^3$	650.
80 W	$4 \cdot 10^{-5}$	0.038	0.022	$8 \cdot 10^{-4}$	$1.7 \cdot 10^3$	1000.
100 W	$5 \cdot 10^{-5}$	0.046	0.025	$10 \cdot 10^{-4}$	$1.45 \cdot 10^3$	790.

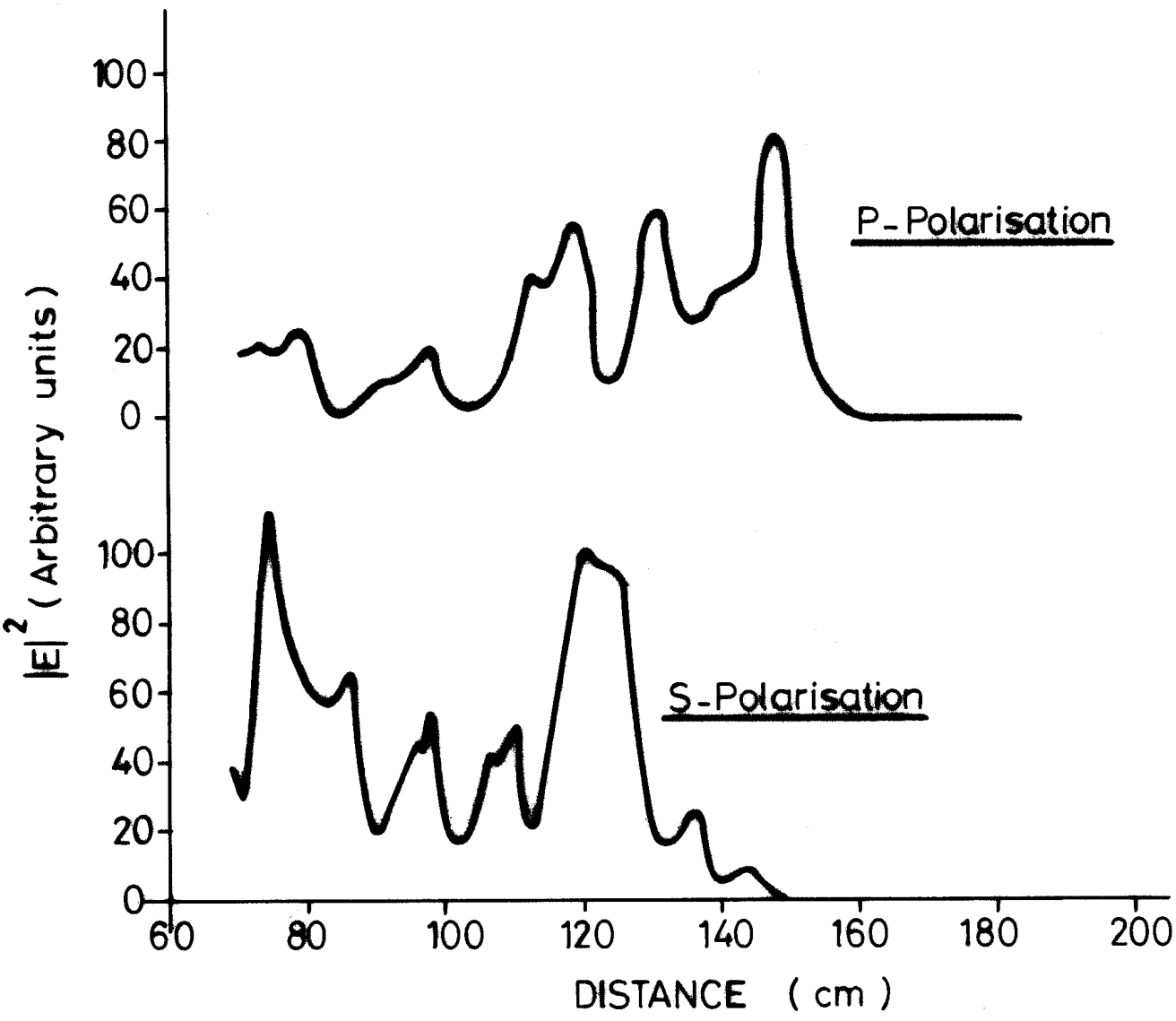
100
80
60
40
20
0
P-Polarisation
100
80
60
40
20
0
S-Polarisation
|E|² (Arbitrary units)
60
80
100
120
140
160
180
200
DISTANCE (cm)

FIGURE 1

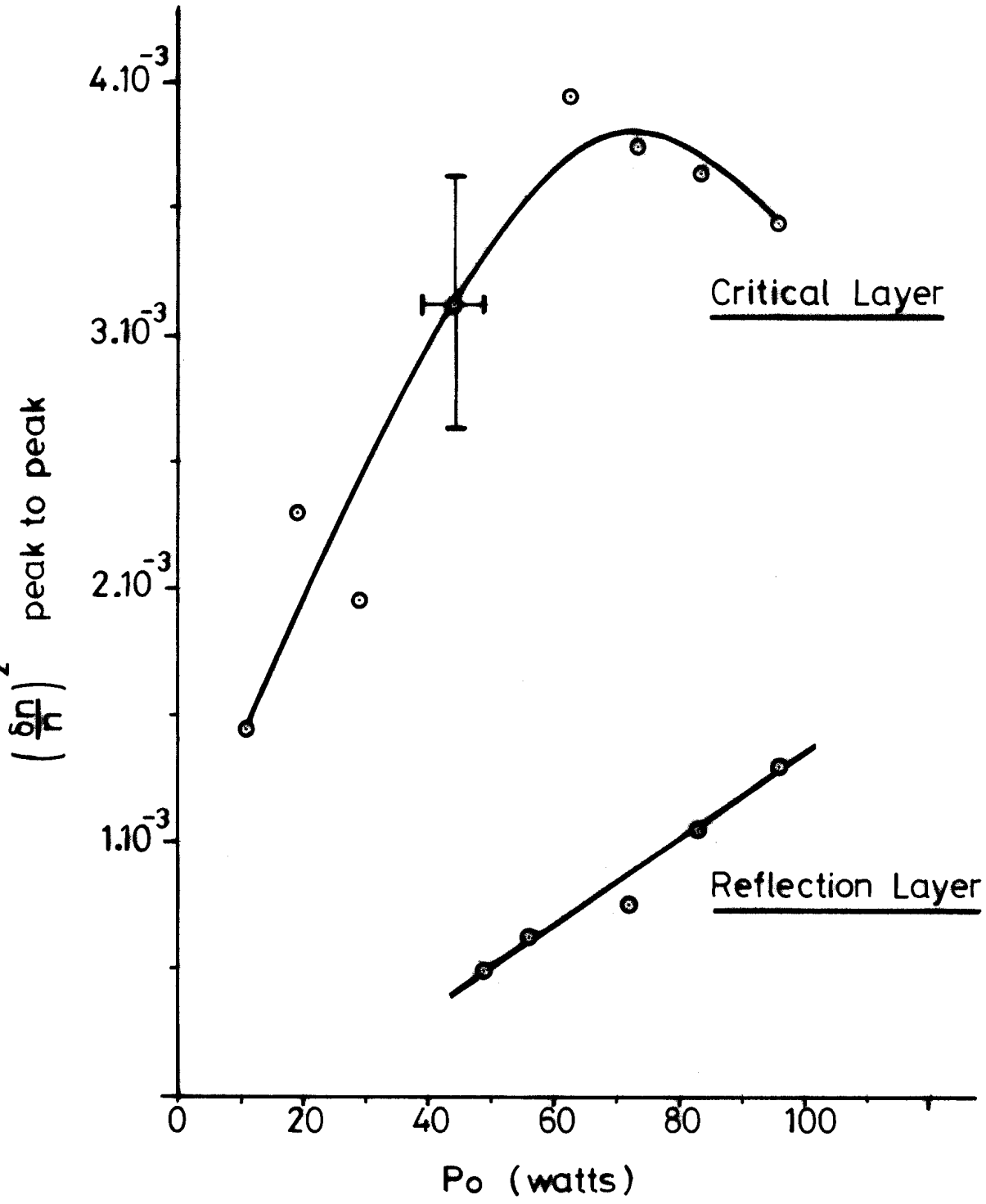
4.10⁻³
3.10⁻³
2.10⁻³
1.10⁻³
(δn/n)² peak to peak
Critical Layer
Reflection Layer
0
20
40
60
80
100
Po (watts)

FIGURE 2

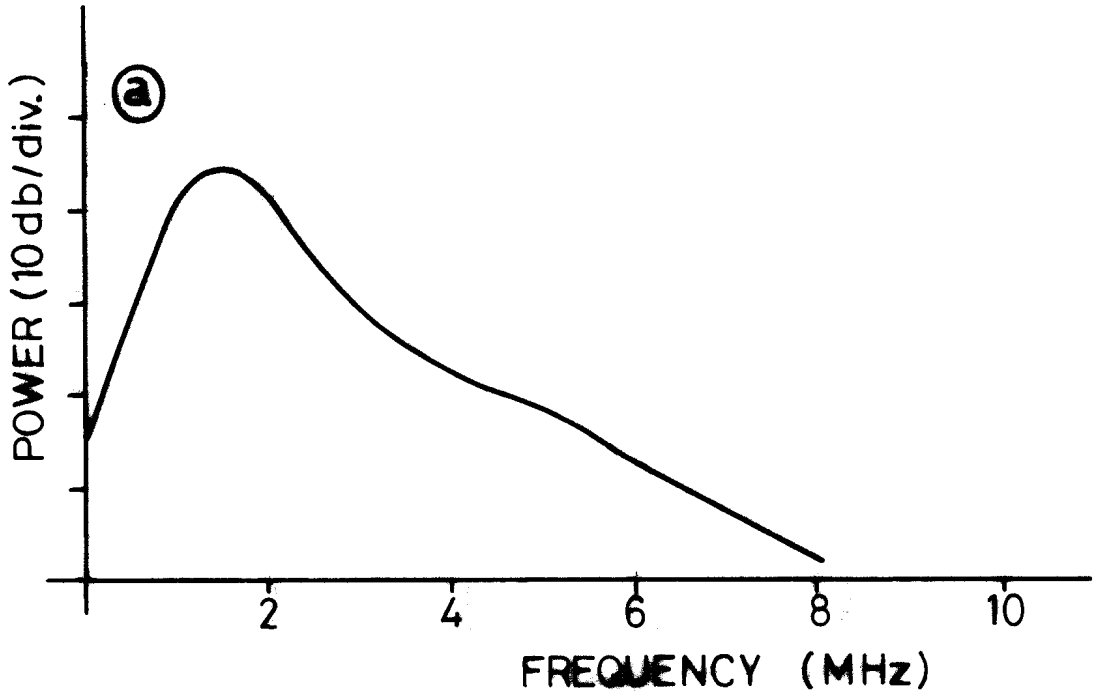
a
POWER (10 db/div.)
2
4
6
8
10
FREQUENCY (MHz)

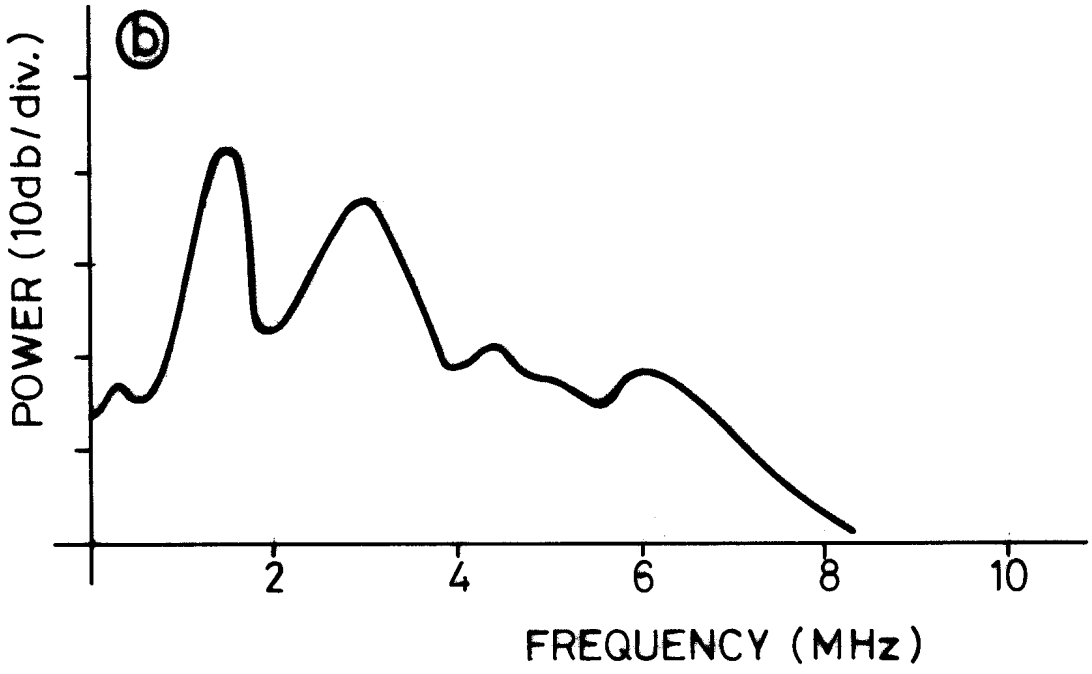
b
POWER (10db/div.)
2
4
6
8
10
FREQUENCY (MHz)

FIGURE 3

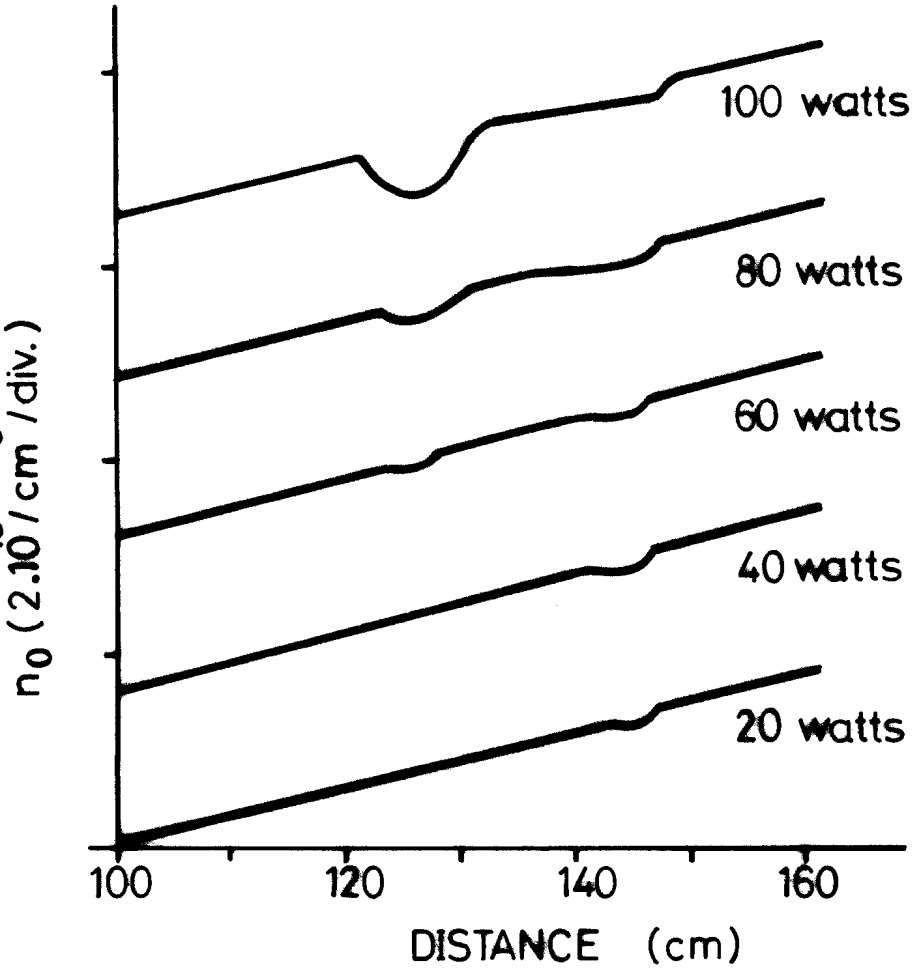
100 watts
80 watts
60 watts
40 watts
20 watts
n_0 (2.10^{10}/cm^3/div.)
100
120
140
160
DISTANCE (cm)

FIGURE 4